HHS Public Access

Author manuscript

Biol Psychiatry. Author manuscript; available in PMC 2016 October 01.

Published in final edited form as:

Biol Psychiatry. 2015 October 1; 78(7): 441–451. doi:10.1016/j.biopsych.2015.02.016.

Gq-DREADD Selectively Initiates Glial Glutamate Release and Inhibits Cue-induced Cocaine Seeking

D. Scofield Michael[1], **A. Boger Heather**[1], **J. Smith Rachel**[1], **Hao Li**[1], **G. Haydon Philip**[2], and **W. Kalivas Peter**[1]

[1]Department of Neurosciences, Medical University of South Carolina Charleston, SC, 29425, USA

[2]Department of Neurosciences, Tufts University, Boston, MA, 02111, USA

Abstract

Background—Glial cells of the central nervous system directly influence neuronal activity by releasing neuroactive small molecules, including glutamate. Long-lasting cocaine-induced reductions in extracellular glutamate in the nucleus accumbens core (NAcore) affect synaptic plasticity responsible for relapse vulnerability.

Methods—We transduced NAcore astrocytes with an AAV viral vector expressing hM3Dq (Gq) DREADD under control of the glial fibrillary acidic protein (GFAP) promoter in 62 male Sprague Dawley rats, 4 dnSNARE mice and 4 wild type littermates. Using glutamate biosensors we measured NAcore glutamate levels following intracranial or systemic administration of clozapine-N-oxide (CNO), and tested the ability of systemic CNO to inhibit reinstated cocaine or sucrose seeking following self-administration (SA) and extinction training.

Results—Administration of CNO in GFAP-Gq-DREADD transfected animals increased NAcore extracellular glutamate levels in vivo. The glial origin of released glutamate was validated by an absence of CNO-mediated release in mice expressing a dominant-negative SNARE variant in glia. Also, CNO-mediated release was relatively insensitive to N-type calcium channel blockade. Systemic administration of CNO inhibited cue-induced reinstatement of cocaine seeking in rats extinguished from cocaine, but not sucrose SA. The capacity to inhibit reinstated cocaine-seeking was prevented by systemic administration of the group II metabotropic glutamate receptor (mGluR2/3) antagonist LY341495.

Conclusions—DREADD-mediated glutamate gliotransmission inhibited cue-induced reinstatement of cocaine seeking by stimulating release-regulating mGluR2/3 autoreceptors to inhibit cue-induced synaptic glutamate spillover.

Address correspondence to: Dr. Michael D. Scofield, Department of Neurosciences, Medical University of South Carolina, 70 President St, Charleston, SC 29403, TEL: 843-876-2246, Scofield@musc.edu.

The authors report no biomedical financial interests or potential conflicts of interest.

Keywords

Cocaine; Glutamate; Astrocytes; DREADD; Reinstatement; Biosensor

Introduction

Addiction is characterized by an enduring vulnerability to relapse mediated by long-lasting drug-induced alterations in glutamatergic synaptic plasticity within the prefrontal cortex (PFC) to nucleus accumbens core (NAcore) circuit (1–3). Animal studies reveal that cocaine exposure reduced levels of basal extracellular glutamate in the NAcore due to decreased glial cystine-glutamate exchange (4, 5). Cocaine-induced reduction of extrasynaptic glutamate tone on presynaptic group II metabotropic glutamate autoreceptors (mGluR2/3) increases synaptic glutamate release probability and contributes to synaptic glutamate spillover during cocaine- or cue-induced reinstatement of cocaine seeking (1, 6, 7). Withdrawal from cocaine exposure also increases expression of the activator of G-protein signaling 3 (AGS3) in the PFC, which selectively binds to Giα-GDP and further inhibits the function of mGluR2/3 (8). Glutamate overflow is then further exacerbated by reduced rates of glutamate clearance that arise from cocaine-induced downregulation of the glial glutamate transporter (GLT-1) (1). These drug-induced perturbations of glutamate homeostasis potentiate glutamatergic synapses in the NAcore and promote excessive glutamate release in response to cue exposure, which induces cocaine-seeking behavior by activating postsynaptic glutamate receptors (1, 9).

Glia maintain basal extracellular glutamate levels required for the regulation of synaptic plasticity by autoreceptors like mGluR2/3 (10). Gliotransmission occurs via several mechanisms including through anion channels, transporters and via Ca^{2+}-dependent release (11, 12). Gliotransmission is likely regulated by intracellular Ca^{2+} ($[Ca^{2+}]_i$) arising from Ca^{2+} stores from the endoplasmic reticulum (ER) and proceeds through a process requiring vesicular Ca^{2+}-dependent binding proteins (13). Studies with Ca^{2+} sensitive dyes reveal oscilliations in astrocytic $[Ca^{2+}]_I$ (14, 15), linked to release of astrocytic transmitters that modulate synaptic transmission and plasticity (13, 16).

We hypothesized that increasing glutamate release from astrocytes before reinstatement would restore tone onto mGluR2/3 autoreceptors, and thereby inhibit the reinstatement of cue-induced cocaine seeking that occurs due to potentiated synaptic release of glutamate. We hypothesized that this manipulation would not drive reinstatement, due to the fact that presynaptic mGluR2/3 autoreceptors are more sensitive to endogenous levels of glutamate then other mGluR subtypes (17, 18). To selectively stimulate astroglial release of Ca^{2+} from intracellular stores, we employed adeno-associated virus (AAV) transduction in the NAcore to express the hM3D (Gq) designer receptor exclusively activated by a designer drug (DREADD) (19, 20) under control of the GFAP promoter (21). Stimulating Gq-coupled DREADDs with clozapine N-oxide (CNO) (20) increases inositol 1,4,5-triphosphate (IP_3) signaling, which increases release of intracellular Ca^{2+} from the ER (21, 22). We employed an in vivo glutamate biosensor to validate CNO-induced release of glutamate into the

extracellular space and demonstrated that glutamate release from astroglia reduces cue-induced cocaine seeking by increasing stimulation of mGluR2/3 autoreceptors.

Methods and Materials

Animal Housing and Surgery

All procedures were conducted in accordance with the National Institutes of Health Guide for the Care and Use of Laboratory Animals and the Association for the Assessment and Accreditation of Laboratory Animal Care International (AAALAC). Male Sprague Dawley rats (250–300 g on arrival; Charles River Laboratories, Wilmington, MA) were individually housed in a temperature- and humidity-controlled environment with a 12 hr dark/light cycle. Experiments were conducted during the animals' dark cycle. Rats received food and water ad libitum and were allowed 1 week to acclimate to the vivarium before surgery. Rats were anesthetized with ketamine HCl (100 mg/kg Ketaset, Fort Dodge Animal Health) and xylazine (10 mg/kg Rompum, Bayer) and given ketorolac analgesic (2 mg/kg Sigma). They were implanted with intravenous jugular catheters, followed by virus microinjections (3, 23). Briefly, 1µl of rAAV5/GFAP-HA-hm3D-IRES-mCitrine (GFAP-Gq-DREADD), (UNC vector core) was infused bilaterally into the NAcore (AP + 1.5 mm; ML ± 1.8 mm; DV − 7.5 mm from bregma, at a 6° angle) using 33 gauge injectors (plastics one) at 0.1µl/min. NAcore AAV transduction was also performed in GFAP promoter driven dominant negative SNARE (dnSNARE) transgenic and wild type littermates utilizing the methods described above, except mice did not receive jugular catheters or undergo cocaine SA. Mice received 0.3µl microinfusion of rAAV5/GFAP-HA-hm3D-IRES-mCitrine (AP +1.1 mm; ML ± 1.2 mm; DV − 4.2 mm from bregma) bilaterally.

Immunohistochemical Staining

Animals were given pentobarbital (200 mg/kg, i.p.) and transcardially perfused 4% formaldehyde. Brains were sliced at 80 µm, and stained for 24 hours with anti-GFAP (Abcam, Cat: ab7260 Lot: GR158671-1), anti-NeuN (Millipore, Cat: MABN140 Lot: 2198089) and/or anti-HA (Covance, Cat: MMS-101P Lot: E12BF00336) antibodies at 1:1000 in PBS + 5% normal goat serum. GFAP, NeuN and HA staining was visualized using Alexa Fluor 488 and 594 (Abcam). Images were obtained with a Leica SP6 confocal (Leica Microsystems). Z-series images were taken at 1–3 micron intervals (see figure S1). For colocalization analyses (Fig 1B,D and Fig 3G), 63X Z-series data sets were imported into Imaris (Bitplane). Once thresholded, a 'colocalization' channel was constructed, which depicts pixels that contain both signals in white, as seen in figures 1B,D and 3G.

Enzyme-Based Microelectrode Array

R2 ceramic-based microelectrode arrays (MEA) were prepared for recordings as described previously (24–26). Briefly, recording sites were coated with a glutamate oxidase (GluOx) (U.S. Biological) containing 1% BSA (Sigma-Aldrich), 0.125% glutaraldehyde (Sigma-Aldrich), and 1% GluOx. 24 hours later, sites were electroplated with an m-Phenylenediamine dihydrochloride (Acros Organics).

Electrode Calibration—Selectivity ratios for glutamate over AA were calculated in addition to the limit of detection (LOD) and linearity (R^2) for all glutamate MEAs (24–26). Electrodes that had R^2 values < 0.99 or had LODs of > 3 μM were excluded. After calibration, MEAs were fitted with single-barrel glass capillaries with an inner tip diameter of ~10 μm. Pipettes were embedded in modeling clay and molten wax was applied to stabilize the assembly. The tip of the pipette was positioned 50 – 100 μm from the surface of the MEA (24, 27). Following attachment, the pipette was filled with 875 μM CNO solution (0.3mg/ml, 0.5% DMSO in 0.9% sterile saline) or a 70 mM KCl solution (70 mM KCl, 79 mM NaCl and 2.5 mM Ca_2Cl, pH 7.4). For ω-conotoxin GVIA experiments and electrochemical experiments using LY341495, a second pipette was positioned 300 μm lateral to the central pipette 50 – 100 μm from the surface of the MEA (Fig. 3A). Effector solution pipettes were filled with 10 μM ω-conotoxin GVIA or with 283 μM LY341495. In all cases, pipettes were connected via tubing to a Picospritzer III (Parker Instruments) for delivery.

Electrode Placement—Rats were anesthetized with 30% urethane at 5 ml/kg and placed in a stereotax (David Kopf Instruments) on a heating pad (37°C). Rats underwent a craniotomy above the NAc and were implanted with MEAs into either the left or right NAcore (AP, +1.8 mm; ML, ±1.5 mm; DV, −7mm versus bregma). Mouse procedures were performed as described above – with the following exceptions. Mice were anesthetized with 15% urethane at 5ml/kg and coordinates used for placement were AP, +1.1 mm; ML, ±1.2 mm; DV, −4.2mm versus bregma.

Recording Procedures—Following implantation, animals underwent 20-min acclimation to establish a stable baseline. *CNO dose-response experiments*: Pressure ejections of 875 μM CNO dissolved in [0.9% sterile saline with 0.5% DMSO] were performed using the Picospritzer III. Fifteen, 30, 60 or 100 nl of CNO solution was ejected ~ 50–100 μm from the surface of the microelectrode to stimulate Gq-DREADD. Following CNO ejection, recordings were allowed to return to baseline for 3–5 minutes before repeating the procedure and/or increasing the amount of CNO ejected. *Intraperitoneal CNO recordings:* Rats were administered either vehicle (1 ml/kg; 5% DMSO in 0.9% sterile saline) or CNO (3 mg/kg, i.p.), recordings were allowed to proceed for one hour following injection of CNO or vehicle. *ω-conotoxin GVIA experiments*: A dual pipette – MEA assembly (Fig. 3A) designed to deliver ω-conotoxin GVIA and either KCl or CNO into the NAcore was constructed. Following application of 60 nL 70 mM KCl recordings were allowed to return to baseline for 3–5 minutes. We then puff applied 60 nL of 10 μM ω-conotoxin GVIA (3.037 ng) immediately followed by application of 60 nL of 70 mM KCl. Maximum glutamate peak height amplitude values were averaged between two and three paired observations for each recording across 4 separate animals. The same procedure was also carried out with 60 nL of 0.3 mg/ml (875 μM) CNO solution substituted for 70 mM KCl in order to evaluate the ability of ω-conotoxin GVIA to inhibit CNO-mediated glutamate release or 60nl of 283 μM LY341495 to evaluate the ability of mGluR2/3 antagonists to impact CNO-mediated glutamate release (Fig. S6). *dnSNARE transgenic mice recordings:* 60 nL of 0.3 mg/ml (875 μM) CNO solution was puff applied as described above in transgenic mice and wild type aged-matched littermates. Maximum glutamate

amplitude was recorded and averaged across 4 CNO applications in 4 dnSNARE transgenic animals and 4 age-matched wild type littermates.

Data Analysis—The FAST16 MKIII recording system saved amperometric data, time, and experimenter ejection marks. All data traces from the MEAs were analyzed using the FAST Analysis software (Jason Burmeister Consulting, LLC). All data were passed through a low stringency wavelet low pass filter (using the Daubechies wavelet).

SA, Extinction and Reinstatement

SA experiments occurred in operant chambers with two levers, a house light, and a cue light and tone (78 dB, 4.5 kHz) generator (Med Associates, Fairfield, VT). During 2-hr sessions, presses on the active lever resulted in a cocaine infusion (0.2 mg in 50 μl, in 0.9% sterile saline) on a fixed ratio 1, with 20 sec timeout; cocaine was provided by National Institute on Drug Abuse. Active lever presses during time out did not result in drug infusion and inactive lever presses had no consequence. Tone and light cues were presented concurrently with the cocaine infusion. Following 10 consecutive SA sessions with >10 infusions, rats began extinction where active lever presses produced no drug infusion or cues. Animals extinguished for 14 days and until < 25 active lever presses were made for 2 days. For cue-induced reinstatement, rats received two i.p. injections of CNO (3 mg/kg, i.p.) or vehicle (0.9% sterile saline with 5% DMSO) at 90 and 30 minutes prior to the reinstatement session. In some experiments, animals also received the mGluR2/3 antagonist LY341495 (1 mg/kg, i.p.) (Tocris) or its vehicle (0.9% sterile saline with 5% DMSO) at the same time they received CNO, according to our previous studies showing blockade of mGluR2/3 with this treatment protocol (28, 29). The reinstatement sessions were identical to a SA session except that pressing the active lever resulted in the presentation of light and tone cues without cocaine delivery. Each rat underwent one reinstatement trial. Sucrose SA, extinction and cued reinstatement were performed in the same manner with 45mg sucrose pellets (Noyes pellets, Fisher Scientific) substituted for cocaine infusions.

Statistics

Reinstatement data were statistically analyzed using a two-way repeated measures ANOVA with a Bonferroni post-test to compare values between treatment groups. Neurochemical measurements were compared using an ANOVA or a Mann-Whitney U test. All statistical tests are conducted using Prism (Graphpad) software.

Results

Astrocyte-specific Expression of Gq-DREADD

Injection of the GFAP-Gq-DREADD virus in the NAcore produced fields of transduced astrocytes, easily distinguished from neurons given their morphology and lack of colocalization with a NeuN neuronal marker (Fig. 1A, B). The GFAP-Gq-DREADD virus produced an immunoreactivity pattern consistent with astrocyte labeling (30–32) and astrocyte-specific expression of Gq-DREADD is very likely given the apparent colocalization of the astrocyte-specific filament protein GFAP and viral HA signals (Fig. 1C, D; see Fig. S1 for individual images of the z-series shown in Fig. 1D; see Fig. S6 for

orthogonal views of Gq-DREADD expression). Gq-DREADD expression was consistently found in ~70% of the GFAP expressing astroglia at the site of virus microinjection (Fig. S2).

Activation of Gq-DREADD with CNO Initiates Glutamate Release

Using in vivo electrochemical recordings, we sampled extracellular glutamate concentrations in real time following CNO administration in animals expressing Gq-DREADD in NAcore astrocytes. Puff application of CNO (875 μM) yielded a reproducible, dose-dependent, transient increase in extracellular glutamate concentration (Fig. 2A, B). Importantly, focal ejections of CNO produced no response when the MEA-pipette assembly was implanted in a control region (dorsal striatum) where viral DREADD expression was absent (Fig. 2A). The dose-dependent increase in the maximum amplitude of glutamate release (μM) versus CNO ejected (pmol) was linear (r^2 = 0.98 +/− 0.03 across 3 separate trials; Fig. 2C). Puff application of the vehicle for CNO (100 nl of 0.9% saline + 0.5% DMSO) produced no glutamate response (Fig. 2B). Systemic injection (i.p.) of vehicle (0.9% saline + 5% DMSO) caused little fluctuation in the baseline levels of glutamate whereas CNO (3 mg/kg, ip) caused an increase in glutamate transients lasting for approximately 60 minutes (representative traces of vehicle and CNO recordings are shown in Fig. 2D). The CNO-mediated glutamate response began approximately 10 minutes after systemic CNO administration (consistent with expected time for CNO to access the brain (19, 33)), was maximal at approximately 20 minutes, and slowly decreased over the next 40 minutes (Fig. 2E).

Low sensitivity of CNO-mediated glutamate release to N-Type Ca^{2+} channel blockade

To verify that DREADD-mediated glial glutamate release was dependent on the release of Ca^{2+} from internal stores, we evaluated the ability of ω-conotoxin GVIA (an N-type Ca^{2+} channel antagonist) to inhibit K^+-mediated and CNO-mediated glutamate release. MEAs were placed in the NAcore with two pipettes fixed to the biosensor, one for 70 mM KCl or 875 μM CNO and another for the application of 10 μM ω-conotoxin GVIA (Fig. 3A). Puff application of 60nl KCl produced peaks with average amplitude of 4.7 μM ± 4.7 and application of 60 nL 875 μM CNO produced peaks with an average amplitude of 2.7 μM ± 2.0 (Fig. 3B, C). Puff application of ω-conotoxin GVIA prior to K^+ application significantly decreased the amplitude of depolarization-induced glutamate peaks to an average of 43% of the K^+ alone response, while ω-conotoxin reduced CNO peaks to 77.5% of the CNO alone maximum amplitude (Fig. 3D). Consistent with a Gq mechanism and the recent report that GFAP driven Gq DREADD activation elevated $[Ca^{2+}]_i$ in astroglia (34), these data indicate that CNO-mediated release of glutamate relies on internal Ca^{2+} stores. Also consistent with this interpretation, previous reports show minor involvement of plasmalemmal Ca^{2+} channel conductances on vescicular glial glutamate release (13, 35).

Genetic inhibition of gliotransmission blocked CNO-mediated glutamate release in the NAcore

To validate CNO-mediated vesicular glutamate release, glutamate MEAs were positioned in fields of GFAP-Gq-DREADD transduced astrocytes in the NAcore of transgenic mice selectively expressing dnSNARE in astrocytes, or in age-matched wild type littermates. The GFAP-Gq-DREADD virus produced an HA immunoreactivity pattern that overlapped

substantially with dnSNARE expression (Figs. 3G and S3). Ejection of 60 nl CNO into dnSNARE transgenic mice produced peak heights of 0.44 μM ± 0.04 whereas application of 60 nl CNO in wild type littermates produced much larger peak heights of 7.27 μM ± 1.93. These results demonstrate that CNO-mediated glutamate release required SNARE-dependent vesicular release.

CNO activation of NAcore glial DREADD inhibited cue-reinstated cocaine seeking via mGluR2/3 activation

To determine whether DREADD-mediated glial glutamate release impacts cue-induced cocaine seeking we employed a rat operant model of cocaine SA followed by extinction training and cued reinstatement (Fig. 4A). Administration of CNO (3 mg/kg, i.p.) 15 minutes prior to a SA session had no effect on the number of active or inactive lever presses compared to a vehicle injection (Fig. 4B). Following extinction, cue-induced reinstatement trials were conducted. Animals were injected with either vehicle or CNO (3 mg/kg) 90 minutes and 30 minutes prior to the reinstatement session. CNO significantly reduced active lever pressing during reinstatement compared to vehicle injection (Fig. 4C), without affecting inactive lever pressing (Fig. S4). Importantly, significant cue-induced reinstatement was observed in non-transduced control animals treated with CNO (Ext = 14 ± 2.4, Reinstatement = 116 ± 28 n=6 paired t-test p=0.015). However, it is important to note that the results from Fig. 4B and C are not directly comparable due to the fact that the CNO treatment paradigm was not identical. To test the hypothesis that the inhibitory effect of CNO was mediated by increased activation of mGluR2/3, reinstatement trials were conducted after animals were given consecutive injections of CNO (3 mg/kg) + LY341495 (1mg/kg), or vehicle + LY341495 (1mg/kg). Rats treated with LY341495 + vehicle displayed significant reinstatement, indicating that blocking mGluR2/3 did not, by itself affect reinstated cocaine seeking (Fig. 4C). However, when LY341495 was administered in concert with CNO the CNO-induced reduction in reinstated lever pressing was reversed (Fig. 4C). To determine if the effect of LY341495 on CNO was caused by inhibiting CNO-induced glutamate release, extracellular glutamate was measured using glutamate biosensors (as described above) and application of LY341495 did not prevent CNO from increasing extracellular glutamate (Fig. S5). Figure 4D shows the location of the injection cannula termination in the NAcore. Stimulating glial glutamate transmission did not produce nonspecific reductions in reinstated operant responding, as we found no effect of CNO treatment on cued reinstatement of sucrose seeking (Fig. 5C; Fig. S4 for inactive lever pressing).

Discussion

Our data demonstrate that Gq-DREADD mediated enhancement of NAcore glial-glutamate release was SNARE-dependent and that the inhibitory effect of glial-glutamate on reinstated cocaine seeking was mediated by mGluR2/3. Several groups have shown that, activation of Gq-DREADD elevates $[Ca^{2+}]_i$, potentially leading to enhanced gliotransmission (21, 34). Here we show that activating Gq-DREADD in NAcore astrocytes promotes the release of glutamate. In support, hippocampal studies reveal a parallel mechanism whereby photolysis of caged astroglial calcium elevated $[Ca^{2+}]_i$, initiated glutamate release, and decreased

synaptic transmission in neighboring neurons by stimulating presynaptic mGluR2/3 (36). Moreover, activation of NAcore mGluR2/3 receptors is an established mechanism to inhibit reinstatement (37–39); however, see (40). In addition, promoting glutamate release into the extracellular space by stimulating cystine-glutamate exchange with N-acetylcysteine also inhibited reinstated cocaine seeking in an mGluR2/3-dependent manner (18, 28). Thus, mGluR2/3 agonists, N-acetylcysteine and GFAP-Gq-DREADD activation inhibit reinstated cocaine seeking by activating presynaptic mGluR2/3 autoreceptors, causing reduced release probability at NAcore synapses (18, 28) (Fig. 6). Further supporting an involvement of glutamate gliotransmission in the regulation of addictive behavior, a recent report from the Bowers lab demonstrated that stimulating glial Gq-DREADD in the NAcore inhibited the motivation to seek ethanol (34). While we used cell morphology and characteristics of glutamate release by CNO (dnSNARE mice and relative insensitivity to N-channel blockers) to show that Gq-DREADD was expressed in glia, a very minor contribution by neuronal Gq-DREADD cannot be 100% ruled out.

Astroglial regulation of synaptic plasticity

Gq-DREADD-mediated NAcore glial glutamate release could also potentially activate extrasynaptic mGluR5, which promotes reinstated cocaine seeking (9, 41). While it is possible that this signaling cascade was engaged, its effects on reinstatement were likely countermanded by the presynaptic actions of Gq-DREADD-mediated glutamate release on mGluR2/3 autoreceptors, which are reported to be more sensitive than other mGluR subtypes (17). Apart from glutamate, activation of Gq signaling in astrocytes and the subsequent increase in $[Ca^{2+}]i$ could also potentially cause release of additional small molecule transmitters including taurine, ATP, and D-serine (11, 12, 42, 43). Despite the fact that the reversal of CNO-mediated inhibition of reinstatement by antagonizing mGluR2/3 indicates the involvement of glutamate, it may be possible that other gliotransmitters contributed to the effect of CNO on reinstated cocaine seeking. As an example, glial release of glutamate and D-serine contribute to the induction of NMDA-dependent slow inward currents, and blocking GluN2B-containing NMDA receptors attenuates both nicotine and heroin seeking (44–46).

dnSNARE Mice

We observed that CNO-mediated (glial) glutamate release was less sensitive to N-type Ca^{2+} channel blockade than K^+ depolarization-mediated (neuronal) glutamate release, consistent with CNO-mediated glutamate release occurring via the mobilization of internal Ca^{2+} from ER stores (47). However, our data also support a partial role for influx of external Ca^{2+}, as CNO-mediated glutamate release was impacted by N-type Ca^{2+} channel blockade. We also observed that CNO-mediated glutamate release in GFAP-dnSNARE transgenic mice was significantly blunted when compared to wild type littermate controls, which is consistent with data shown by others demonstrating inhibited hippocampal glial adenosine release in GFAP-dnSNARE mice (48). Interestingly, the GFAP dnSNARE mice did not display cue-induced reinstatement of cocaine seeking (49). This suggests that while increasing glial release of glutamate locally in the NAcore inhibits reinstated cocaine seeking, a global loss of gliotransmission impairs reinstated cocaine seeking (49).

As is the case with any model, the tTA-tetO based dnSNARE transgenic mice have potential caveats including chromosomal positioning effects and the possibility of leaky transgene expression from the tTA-tetO system. Contrary to what we observed in the NAcore, a recent report indicates that the dnSNARE mice show off target neuronal expression of the dnSNARE transgene in the cerebral cortex (50). These results provoke further debate on astrocytic Ca^{2+}-dependent vesicular exocytosis, and highlight that additional examination of the dnSNARE model is required to determine its usefulness moving forward.

Ca^{2+} dependent release of glutamate from astroglia

There are several mechanisms that astrocytes utilize to release neuroactive molecules (10), with Ca^{2+}-dependent vesicular exocytosis being one of the more debated and intriguing modalities (13). In light of the oscillation of $[Ca^{2+}]_i$ observed in astrocytes (51), gliotransmission is thought to occur via the mobilization of internal calcium stores, most likely as a result of the activation of Gq signaling and the production of the second messenger IP_3 (13). Several studies support the role of astroglial IP_3 signaling in the modulation of synaptic plasticity by glial cells (52, 53), yet others report a lack of IP_3-mediated effects on synaptic activity (54). However, there is general consensus that transmitters released from astrocytes can alter synaptic activity (36, 55–57), and that astrocytes express the vesicular glutamate transporter and synthesize the proteins necessary for the assembly of the SNARE complex required for vesicle fusion (16, 58–60). In the work presented above, it is interesting that the increased levels of glutamate observed over the 60 minutes after systemic CNO administration were composed of transients, reminiscent of quantal release events. Clearly the time course of the CNO-induced glutamate transients exceeded expectations for synaptic quanta (61), implying either a more prolonged fusion-release process than synaptic vesicular release or an accumulation of glutamate from the closely timed release of glutamate from multiple glial vesicles. Unfortunately, the sensitivity of the biosensors (~1 μM) does not permit a more detailed quantification of the glutamate transients.

Investigations of exocytotic release of glutamate from astrocytes and its role as a signaling mechanism have been contradictory. Woo and colleagues have shown that astroglial activation of Gq-coupled receptors induces slow, non-vesicular glutamate release in hippocampal astrocytes through the glutamate-permeable Ca^{2+}-activated anion channel Best1 (62). However, recent reports provide evidence supporting vesicular release of ATP in response to elevations of $[Ca^{2+}]_i$ (60). Lalo and colleagues observed a diminished burst of purinergic currents using sniffer cell technology following PAR-1 receptor (Gq) activation when slices were taken from dnSNARE mice, indicating that Ca^{2+}-mediated release of ATP occurs through SNARE-dependent vesicular exocytosis (60). Recent data from this group also supports vesicular release of glutamate from astrocytes whereby elevation of $[Ca^{2+}]_i$ resulted in NMDA-receptor mediated mEPSCs that were absent in slices prepared from dnSNARE mice (63). Additional experimentation is required in order to characterize precisely which signaling cascades are responsible for increasing $[Ca^{2+}]_I$, how this mechanistically leads to the release of glutamate, and if there are differences in the mechanisms underlying Ca^{2+}-mediated gliotransmission across brain regions.

Conclusions

Our study demonstrates that the acute release of glutamate from glia can inhibit cue-induced reinstatement of cocaine seeking in an mGluR2/3-dependent manner. As such, mGluR2/3 agonists appear an attractive target for cocaine relapse prevention medication. However, most studies have shown that mGluR2/3 agonists also decrease other motivated behaviors, such as food seeking (37, 64, 65); although this was not seen with a positive allosteric mGluR2/3 agonist (38). The fact that there was no effect on sucrose reinstatement following Gq-DREADD activation poses the possibility that stimulating mGluR2/3 selectively by enhancing glial glutamate release at a specific site of pathology in the brain (i.e. the NAcore) may yield a pharmacogenetic therapy lacking the side-effects elicited by direct small molecule mGluR2/3 agonists that would act throughout the brain.

Supplementary Material

Refer to Web version on PubMed Central for supplementary material.

Acknowledgments

This research was supported by grants from the National Institute of Health to PWK (R015369 and DA003906). MDS was also partially supported by a National Institute on Drug Abuse training grant (T32 DA 7288-22).

References

1. Kalivas PW. The glutamate homeostasis hypothesis of addiction. Nat Rev Neurosci. 2009; 10:561–572. [PubMed: 19571793]
2. Goldstein RZ, Volkow ND. Drug addiction and its underlying neurobiological basis: neuroimaging evidence for the involvement of the frontal cortex. Am J Psychiatry. 2002; 159:1642–1652. [PubMed: 12359667]
3. Stefanik MT, Moussawi K, Kupchik YM, Smith KC, Miller RL, Huff ML, et al. Optogenetic inhibition of cocaine seeking in rats. Addict Biol. 2013; 18:50–53. [PubMed: 22823160]
4. Reissner KJ, Kalivas PW. Using glutamate homeostasis as a target for treating addictive disorders. Behav Pharmacol. 2010; 21:514–522. [PubMed: 20634691]
5. Baker DA, McFarland K, Lake RW, Shen H, Tang XC, Toda S, et al. Neuroadaptations in cystine-glutamate exchange underlie cocaine relapse. Nat Neurosci. 2003; 6:743–749. [PubMed: 12778052]
6. Moussawi K, Kalivas PW. Group II metabotropic glutamate receptors (mGlu2/3) in drug addiction. Eur J Pharmacol. 2010; 639:115–122. [PubMed: 20371233]
7. Knackstedt LA, Kalivas PW. Glutamate and reinstatement. Curr Opin Pharmacol. 2009; 9:59–64. [PubMed: 19157986]
8. Bowers MS, McFarland K, Lake RW, Peterson YK, Lapish CC, Gregory ML, et al. Activator of G protein signaling 3: a gatekeeper of cocaine sensitization and drug seeking. Neuron. 2004; 42:269–281. [PubMed: 15091342]
9. Wang X, Moussawi K, Knackstedt L, Shen H, Kalivas PW. Role of mGluR5 neurotransmission in reinstated cocaine-seeking. Addict Biol. 2013; 18:40–49. [PubMed: 22340009]
10. Scofield MD, Kalivas PW. Astrocytic Dysfunction and Addiction: Consequences of Impaired Glutamate Homeostasis. Neuroscientist. 2014
11. Halassa MM, Haydon PG. Integrated brain circuits: astrocytic networks modulate neuronal activity and behavior. Annual review of physiology. 2010; 72:335–355.
12. Parpura V, Zorec R. Gliotransmission: Exocytotic release from astrocytes. Brain Res Rev. 2009; 63:83–92. [PubMed: 19948188]
13. Zorec R, Araque A, Carmignoto G, Haydon PG, Verkhratsky A, Parpura V. Astroglial excitability and gliotransmission: an appraisal of Ca2+ as a signalling route. ASN Neuro. 2012; 4

14. Cornell-Bell AH, Finkbeiner SM, Cooper MS, Smith SJ. Glutamate induces calcium waves in cultured astrocytes: long-range glial signaling. Science. 1990; 247:470–473. [PubMed: 1967852]
15. Dani JW, Chernjavsky A, Smith SJ. Neuronal activity triggers calcium waves in hippocampal astrocyte networks. Neuron. 1992; 8:429–440. [PubMed: 1347996]
16. Martineau M, Shi T, Puyal J, Knolhoff AM, Dulong J, Gasnier B, et al. Storage and uptake of D-serine into astrocytic synaptic-like vesicles specify gliotransmission. J Neurosci. 2013; 33:3413–3423. [PubMed: 23426669]
17. Cartmell J, Schoepp DD. Regulation of neurotransmitter release by metabotropic glutamate receptors. J Neurochem. 2000; 75:889–907. [PubMed: 10936169]
18. Kupchik YM, Moussawi K, Tang XC, Wang X, Kalivas BC, Kolokithas R, et al. The effect of N-acetylcysteine in the nucleus accumbens on neurotransmission and relapse to cocaine. Biol Psychiatry. 2012; 71:978–986. [PubMed: 22137594]
19. Rogan SC, Roth BL. Remote control of neuronal signaling. Pharmacol Rev. 2011; 63:291–315. [PubMed: 21415127]
20. Armbruster BN, Li X, Pausch MH, Herlitze S, Roth BL. Evolving the lock to fit the key to create a family of G protein-coupled receptors potently activated by an inert ligand. Proc Natl Acad Sci USA. 2007; 104:5163–5168. [PubMed: 17360345]
21. Agulhon C, Boyt KM, Xie AX, Friocourt F, Roth BL, McCarthy K. Modulation of the autonomic nervous system by acute glial cell Gq-GPCR activation in vivo. J Physiol. 2013
22. Sasaki K, Suzuki M, Mieda M, Tsujino N, Roth B, Sakurai T. Pharmacogenetic modulation of orexin neurons alters sleep/wakefulness states in mice. PLoS One. 2011; 6:e20360. [PubMed: 21647372]
23. Stefanik MT, Kalivas PW. Optogenetic dissection of basolateral amygdala projections during cue-induced reinstatement of cocaine seeking. Frontiers in behavioral neuroscience. 2013; 7:213. [PubMed: 24399945]
24. Burmeister JJ, Pomerleau F, Palmer M, Day BK, Huettl P, Gerhardt GA. Improved ceramic-based multisite microelectrode for rapid measurements of L-glutamate in the CNS. J Neurosci Methods. 2002; 119:163–171. [PubMed: 12323420]
25. Quintero JE, Pomerleau F, Huettl P, Johnson KW, Offord J, Gerhardt GA. Methodology for rapid measures of glutamate release in rat brain slices using ceramic-based microelectrode arrays: basic characterization and drug pharmacology. Brain Res. 2011; 1401:1–9. [PubMed: 21664606]
26. Onifer SM, Quintero JE, Gerhardt GA. Cutaneous and electrically evoked glutamate signaling in the adult rat somatosensory system. J Neurosci Methods. 2012; 208:146–154. [PubMed: 22627377]
27. Michael, AC.; Borland, LM. Electrochemical methods for neuroscience. Boca Raton: CRC Press/ Taylor & Francis; 2007.
28. Moran MM, McFarland K, Melendez RI, Kalivas PW, Seamans JK. Cystine/glutamate exchange regulates metabotropic glutamate receptor presynaptic inhibition of excitatory transmission and vulnerability to cocaine seeking. J Neurosci. 2005; 25:6389–6393. [PubMed: 16000629]
29. Moussawi K, Riegei A, Nair S, Kalivas PW. Extracellular glutamate: functional compartments operate in different concentration ranges. Front Syst Neurosci. 2011; 5:94. [PubMed: 22275885]
30. Bushong EA, Martone ME, Jones YZ, Ellisman MH. Protoplasmic astrocytes in CA1 stratum radiatum occupy separate anatomical domains. J Neurosci. 2002; 22:183–192. [PubMed: 11756501]
31. Benediktsson AM, Schachtele SJ, Green SH, Dailey ME. Ballistic labeling and dynamic imaging of astrocytes in organotypic hippocampal slice cultures. J Neurosci Methods. 2005; 141:41–53. [PubMed: 15585287]
32. Morel L, Higashimori H, Tolman M, Yang Y. VGluTl+ neuronal glutamatergic signaling regulates postnatal developmental maturation of cortical protoplasmic astroglia. J Neurosci. 2014; 34:10950–10962. [PubMed: 25122895]
33. Alexander GM, Rogan SC, Abbas AI, Armbruster BN, Pei Y, Allen JA, et al. Remote control of neuronal activity in transgenic mice expressing evolved G protein-coupled receptors. Neuron. 2009; 63:27–39. [PubMed: 19607790]

34. Bull C, Freitas KC, Zou S, Poland RS, Syed WA, Urban DJ, et al. Rat Nucleus Accumbens Core Astrocytes Modulate Reward and the Motivation to Self-Administer Ethanol after Abstinence. Neuropsychopharmacology. 2014
35. Parri HR, Crunelli V. The role of Ca2+ in the generation of spontaneous astrocytic Ca2+ oscillations. Neuroscience. 2003; 120:979–992. [PubMed: 12927204]
36. Liu QS, Xu Q, Rang J, Nedergaard M. Astrocyte activation of presynaptic metabotropic glutamate receptors modulates hippocampal inhibitory synaptic transmission. Neuron glia biology. 2004; 1:307–316. [PubMed: 16755304]
37. Peters J, Kalivas PW. The group II metabotropic glutamate receptor agonist, LY379268, inhibits both cocaine- and food-seeking behavior in rats. Psychopharmacology (Berl). 2006; 186:143–149. [PubMed: 16703399]
38. Jin X, Semenova S, Yang L, Ardecky R, Sheffler DJ, Dahl R, et al. The mGluR2 positive allosteric modulator BINA decreases cocaine self-administration and cue-induced cocaine-seeking and counteracts cocaine-induced enhancement of brain reward function in rats. Neuropsychopharmacology. 2010; 35:2021–2036. [PubMed: 20555310]
39. Hao Y, Martin-Fardon R, Weiss F. Behavioral and functional evidence of metabotropic glutamate receptor 2/3 and metabotropic glutamate receptor 5 dysregulation in cocaine-escalated rats: factor in the transition to dependence. Biol Psychiatry. 2010; 68:240–248. [PubMed: 20416862]
40. Bauzo RM, Kimmel HL, Howell LL. Interactions between the mGluR2/3 agonist, LY379268, and cocaine on in vivo neurochemistry and behavior in squirrel monkeys. Pharmacol Biochem Behav. 2009; 94:204–210. [PubMed: 19703487]
41. Moussawi K, Pacchioni A, Moran M, Olive MF, Gass JT, Lavin A, et al. N-Acetylcysteine reverses cocaine-induced metaplasticity. Nat Neurosci. 2009; 12:182–189. [PubMed: 19136971]
42. Agulhon C, Sun MY, Murphy T, Myers T, Lauderdale K, Fiacco TA. Calcium Signaling and Gliotransmission in Normal vs. Reactive Astrocytes. Front Pharmacol. 2012; 3:139. [PubMed: 22811669]
43. Choe KY, Olson JE, Bourque CW. Taurine release by astrocytes modulates osmosensitive glycine receptor tone and excitability in the adult supraoptic nucleus. J Neurosci. 2012; 32:12518–12527. [PubMed: 22956842]
44. Fellin T, D'Ascenzo M, Haydon PG. Astrocytes control neuronal excitability in the nucleus accumbens. The Scientific World Journal. 2007; 7:89–97. [PubMed: 17982581]
45. Shen H, Moussawi K, Zhou W, Toda S, Kalivas PW. Heroin relapse requires long-term potentiation-like plasticity mediated by NMDA2b-containing receptors. Proc Natl Acad Sci USA. 2011; 108:19407–19412. [PubMed: 22084102]
46. Gipson CD, Reissner KJ, Kupchik YM, Smith AC, Stankeviciute N, Hensley-Simon ME, et al. Reinstatement of nicotine seeking is mediated by glutamatergic plasticity. Proc Natl Acad Sci USA. 2013; 110:9124–9129. [PubMed: 23671067]
47. Horne AL, Kemp JA. The effect of omega-conotoxin GVIA on synaptic transmission within the nucleus accumbens and hippocampus of the rat in vitro. Br J Pharmacol. 1991; 103:1733–1739. [PubMed: 1657265]
48. Schmitt LI, Sims RE, Dale N, Haydon PG. Wakefulness affects synaptic and network activity by increasing extracellular astrocyte-derived adenosine. J Neurosci. 2012; 32:4417–4425. [PubMed: 22457491]
49. Turner JR, Ecke LE, Briand LA, Haydon PG, Blendy JA. Cocaine-related behaviors in mice with deficient gliotransmission. Psychopharmacology (Berl). 2012; 226:167–176. [PubMed: 23104263]
50. Fujita T, Chen MJ, Li B, Smith NA, Peng W, Sun W, et al. Neuronal Transgene Expression in Dominant-Negative SNARE Mice. J Neurosci. 2014; 34:16594–16604. [PubMed: 25505312]
51. Dani JW, Smith SJ. The triggering of astrocytic calcium waves by NMDA-induced neuronal activation. Ciba Foundation symposium. 1995; 188:195–205. discussion 205–199. [PubMed: 7587618]
52. Navarrete M, Perea G, Fernandez de Sevilla D, Gomez-Gonzalo M, Nunez A, Martin ED, et al. Astrocytes mediate in vivo cholinergic-induced synaptic plasticity. PLoS biology. 2012; 10:e1001259. [PubMed: 22347811]

53. Takata N, Mishima T, Hisatsune C, Nagai T, Ebisui E, Mikoshiba K, et al. Astrocyte calcium signaling transforms cholinergic modulation to cortical plasticity in vivo. J Neurosci. 2011; 31:18155–18165. [PubMed: 22159127]
54. Petravicz J, Fiacco TA, McCarthy KD. Loss of IP3 receptor-dependent Ca2+ increases in hippocampal astrocytes does not affect baseline CAI pyramidal neuron synaptic activity. J Neurosci. 2008; 28:4967–4973. [PubMed: 18463250]
55. Santello M, Cali C, Bezzi P. Gliotransmission and the tripartite synapse. Advances in experimental medicine and biology. 2012; 970:307–331. [PubMed: 22351062]
56. Theodosis DT, Poulain DA, Oliet SH. Activity-dependent structural and functional plasticity of astrocyte-neuron interactions. Physiol Rev. 2008; 88:983–1008. [PubMed: 18626065]
57. Pirttimaki TM, Hall SD, Parri HR. Sustained neuronal activity generated by glial plasticity. J Neurosci. 2011; 31:7637–7647. [PubMed: 21613477]
58. Montana V, Ni Y, Sunjara V, Hua X, Parpura V. Vesicular glutamate transporter-dependent glutamate release from astrocytes. J Neurosci. 2004; 24:2633–2642. [PubMed: 15028755]
59. Calegari F, Coco S, Taverna E, Bassetti M, Verderio C, Corradi N, et al. A regulated secretory pathway in cultured hippocampal astrocytes. J Biol Chem. 1999; 274:22539–22547. [PubMed: 10428831]
60. Lalo U, Palygin O, Rasooli-Nejad S, Andrew J, Haydon PG, Pankratov Y. Exocytosis of ATP from astrocytes modulates phasic and tonic inhibition in the neocortex. PLoS biology. 2014; 12:e1001747. [PubMed: 24409095]
61. Katz B. Quantal mechanism of neural transmitter release. Science. 1971; 173:123–126. [PubMed: 4325812]
62. Woo DH, Han KS, Shim JW, Yoon BE, Kim E, Bae JY, et al. TREK-1 and Bestl channels mediate fast and slow glutamate release in astrocytes upon GPCR activation. Cell. 2012; 151:25–40. [PubMed: 23021213]
63. Rasooli-Nejad, S.; Lalo, U.; Pankratov, Y. Exocytosis of gliotransmitters from astrocytes and its implications for synaptic plasticity in the neocortex. Society for Neuroscience; San Diego, CA: 2013.
64. Bossert JM, Gray SM, Lu L, Shaham Y. Activation of group II metabotropic glutamate receptors in the nucleus accumbens shell attenuates context-induced relapse to heroin seeking. Neuropsychopharmacology. 2006; 31:2197–2209. [PubMed: 16341024]
65. Baptista MA, Martin-Fardon R, Weiss F. Preferential effects of the metabotropic glutamate 2/3 receptor agonist LY379268 on conditioned reinstatement versus primary reinforcement: comparison between cocaine and a potent conventional reinforcer. J Neurosci. 2004; 24:4723–4727. [PubMed: 15152032]

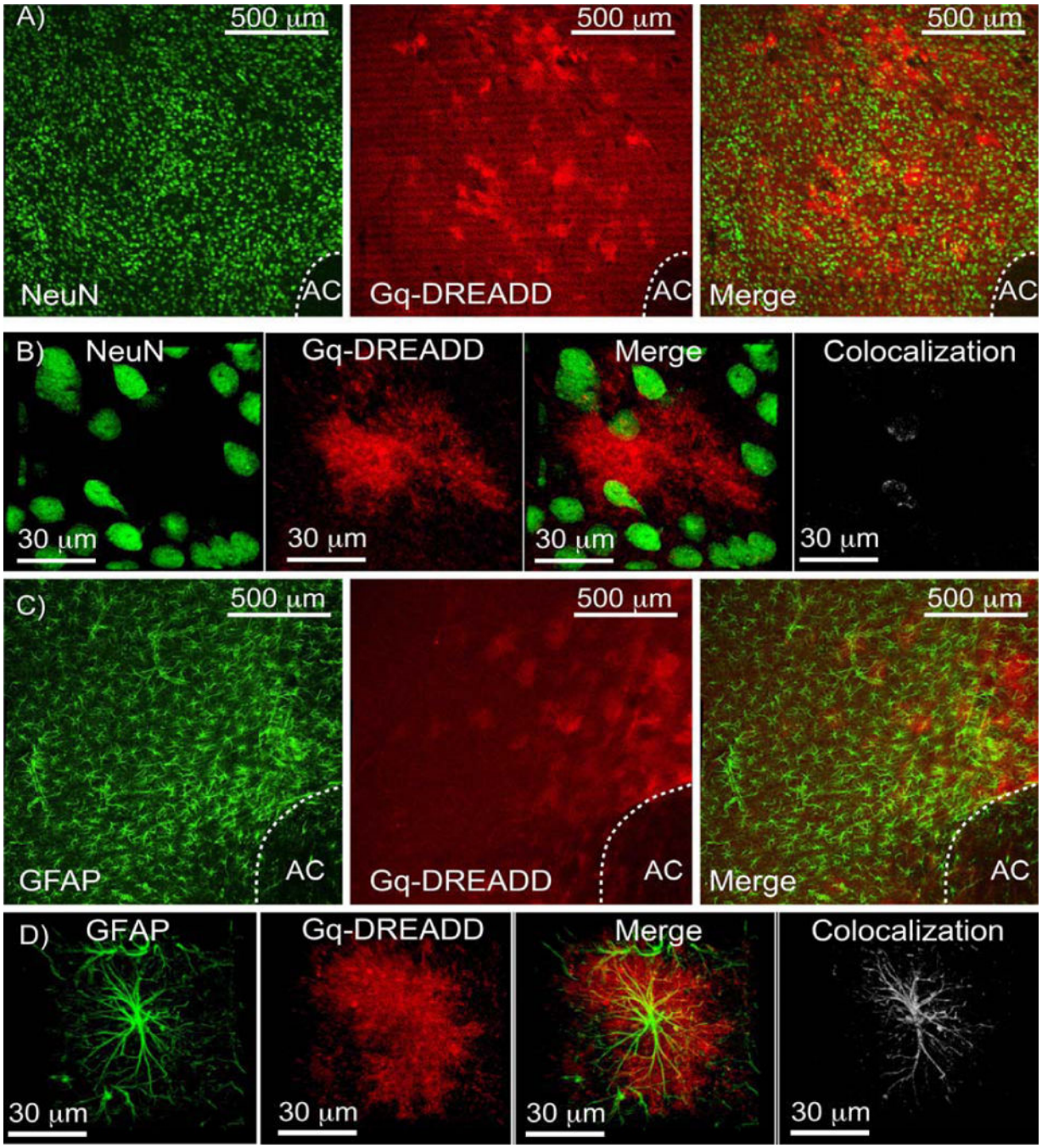

Figure 1. Astrocyte-specific expression of Gq-DREADD

A) 10X Z-series images of a field of cells containing the accumbens with NeuN labeling in green, viral DREADD expression (HA tag) in red and a red-green merged image. In each image the anterior commissure is labeled "AC". **B)** 63X Z-series images of NeuN in green, viral DREADD expression (HA tag) in red, a merged image and a 3D colocalization channel built by Imaris. 3D colocalization analysis shows very little co-labeling (white) of the viral HA and NeuN signals. **(C)** 10X Z-series images of a field of cells containing the accumbens with GFAP labeling in green and viral DREADD expression (HA tag) in red as well as a

merged image. **(D)** 63X Z-series images with GFAP in green and viral DREADD expression (HA tag) in red along with a merged image and a 3D colocalization channel built by Imaris (white). Here 3D colocalization analysis displays co-labeling of the astrocyte-specific GFAP intermediate filament protein with viral HA staining.

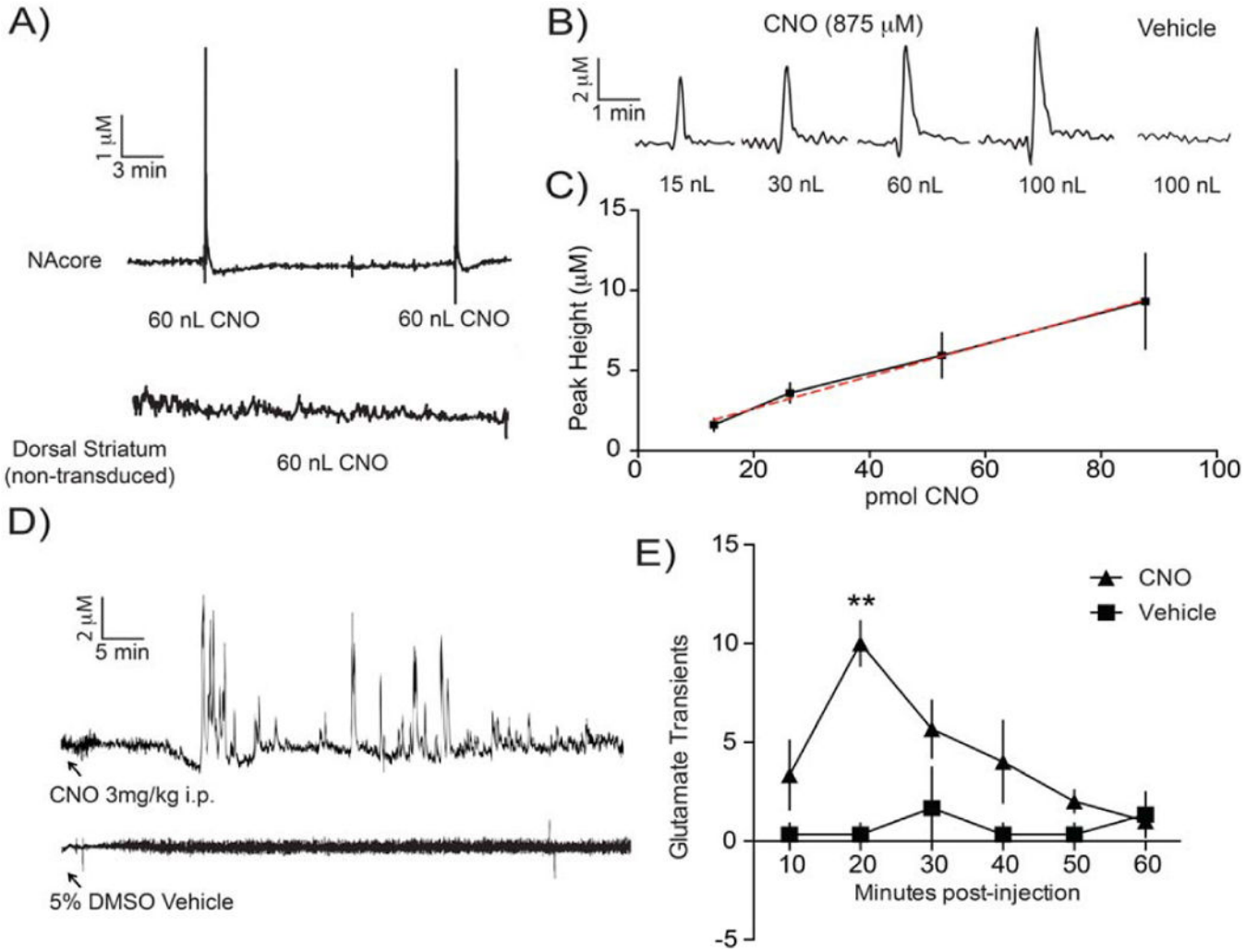

Figure 2. Activation of glial-DREADDs with CNO initiated glutamate release

A) Representative glutamate peaks elicited by CNO puff application in the NAcore and the lack of a response in the dorsal striatum (non-transduced control region). **B)** Representative glutamate peaks elicited by puff application of increasing amounts of CNO **C)** Graph of maximum glutamate peak amplitude in μM vs pmol of CNO ejected, n=3 animals. **D)** Top, following an i.p. injection of 3 mg/kg CNO, glutamate spiking is observed for approximately 60 minutes. Bottom, vehicle recording shows very little activity in the NAc after an injection of 1ml/kg saline + 5% DMSO. **E)** CNO induced glutamate spiking following i.p. administration was quantified as number of peaks per 10 min, with a peak defined as having an amplitude >3-times the height of the variability in the baseline recording. n= 3 each for CNO and vehicle. Two way repeated measures ANOVA revealed a significant effect of CNO treatment ($F_{(1, 2)}$=25; p=0.038), time ($F_{(5, 10)}$=5.602; p=0.10) and a significant interaction ($F_{(5, 10)}$=3.950, p=0.031). Bonferroni posttests revealed that glutamate transients were significantly higher at 20 minutes after CNO injection when compared to vehicle, ** p<0.01.

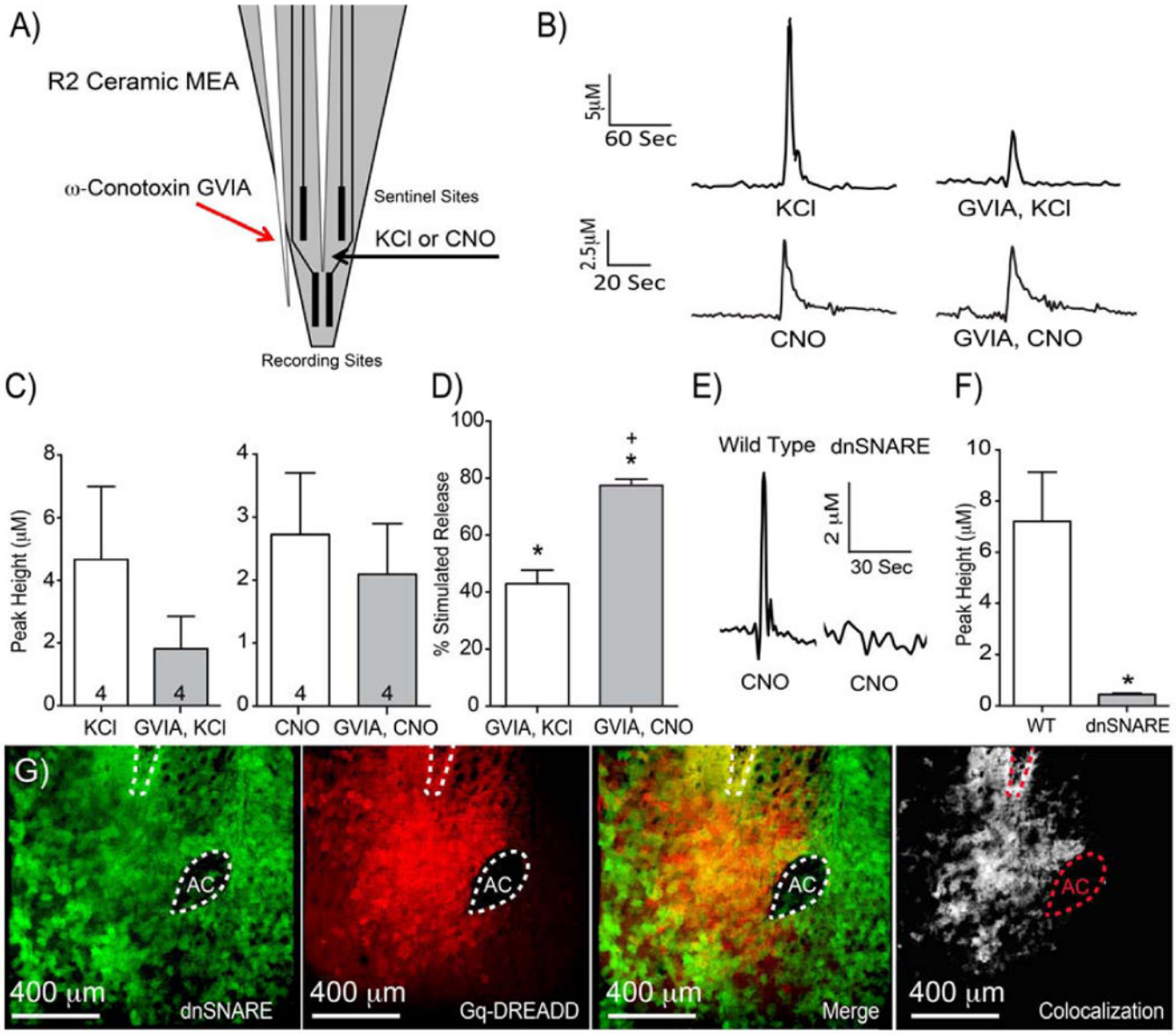

Figure 3. CNO-mediated glutamate release was less sensitive to N-Type Ca^{2+} channel blockade than K^+-mediated glutamate release and required SNARE-dependent gliotransmission

A) A schematic of the dual pipette MEA assembly depicting which pipette contained each solution. **B)** Representative traces of KCl and CNO peaks with and without GVIA inhibition. For all solutions ejection volumes were 60 nl. **C)** Left, maximum peak height for KCl experiments. Right, maximum peak height for CNO experiments. For both KCl and CNO experiments, peak heights from 2–3 matched observations were averaged across 4 separate animals. **D)** Percentage of the uninhibited prior response is shown for both KCl and CNO experiments. ω-conotoxin GVIA significantly reduced peak height of K^+-mediated release (one sample t-test *p=0.0012) as well as CNO-mediated release (one sample t-test *p=0.0019). K^+-mediated glutamate release was more sensitive to ω-conotoxin GVIA than CNO-mediated glutamate release, Mann-Whitney test +p=0.029. **E)** Representative 60 nl CNO peaks in wild type and dnSNARE transgenic animals with GFAP-Gq-DREADD

expression in the NAcore. **F)** Maximum amplitude of CNO-mediated glutamate release in dnSNARE transgenic mice and wild type littermates. Maximum amplitude of 4 CNO peaks was averaged and across 4 separate animals for both wild type and dnSNARE transgenics. Glutamate peak height was significantly higher in wild type littermates when compared to dnSNARE transgenic mice Mann-Whitney test * p=0.029. **G)** Gq-DREADD viral expression, dnSNARE expression and MEA placement were confirmed ex-vivo using Z-series confocal imaging. The representative micrographs depict dnSNARE in green, viral transduction of NAcore astrocytes with Gq-DREADD in red, a merged image, and a 3D colocalization analysis of the 2 signals in white. White signal shows the 3D co-registration of the Gq-DREADD and dnSNARE signals in the z-series. In these images the anterior commissure is labeled “AC’ and is surrounded by a broken white line and the damage created by the MEA probe, located in a field of virally transduced cells, is also surrounded by a broken white line.

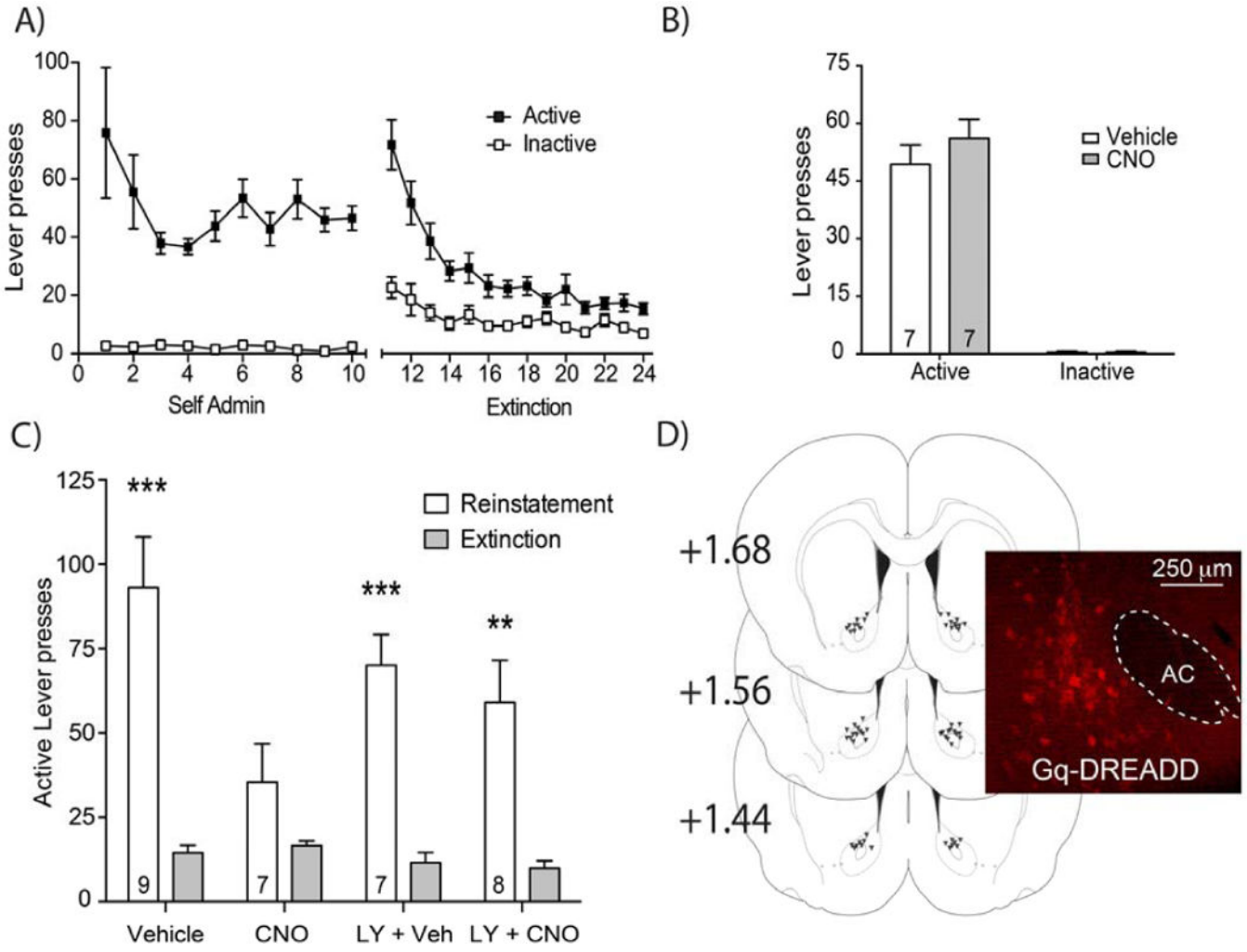

Figure 4. Activation of Gq signaling in astrocytes inhibited cue-induced cocaine reinstatement via mGluR2/3

A) Cocaine SA and extinction data (X-axis is days). **B)** Two-way repeated measures ANOVA revealed no significant effect of i.p. injection of CNO on active or inactive lever pressing during cocaine SA ($F_{(1, 12)}$=2.575; p=0.135), a significant difference between active and inactive lever presses ($F_{(1, 12)}$=132.6; p<0.0001) and no interaction ($F_{(1, 12)}$=2.575; p=0.1346). Bonferroni posttests revealed no significant differences in active vs inactive lever presses in CNO and vehicle treated animals, p>0.05 **C)** Active lever presses for extinction and reinstatement for Vehicle, CNO, LY341495 and LY341495 + CNO groups. Two-way repeated measures ANOVA revealed a significant effect of treatment ($F_{(3, 27)}$=3.126; p=0.042), significant effect of reinstatement ($F_{(1, 27)}$=70.5, p<0.0001) and a significant interaction ($F_{(3, 27)}$=4.174, p=0.015). Bonferroni posttests revealed that cue-induced reinstatement increased active lever pressing significantly (compared to extinction) in the vehicle control group, as well as in the LY341495 and LY341495 + CNO groups but not in the CNO group, ** p<0.01, *** p<0.001. **D)** injection sites for rAAV5/GFAP-HA-hm3D-IRES-mCitrine viral infusion. The terminal point of the injection sites are represented as small black triangles with the coordinates shown relative to bregma. The representative

micrograph shown details the location of the tip of the injection cannula relative to the anterior commissure (ac) and expression of the viral HA tag. *p< 0.05, compared to extinction

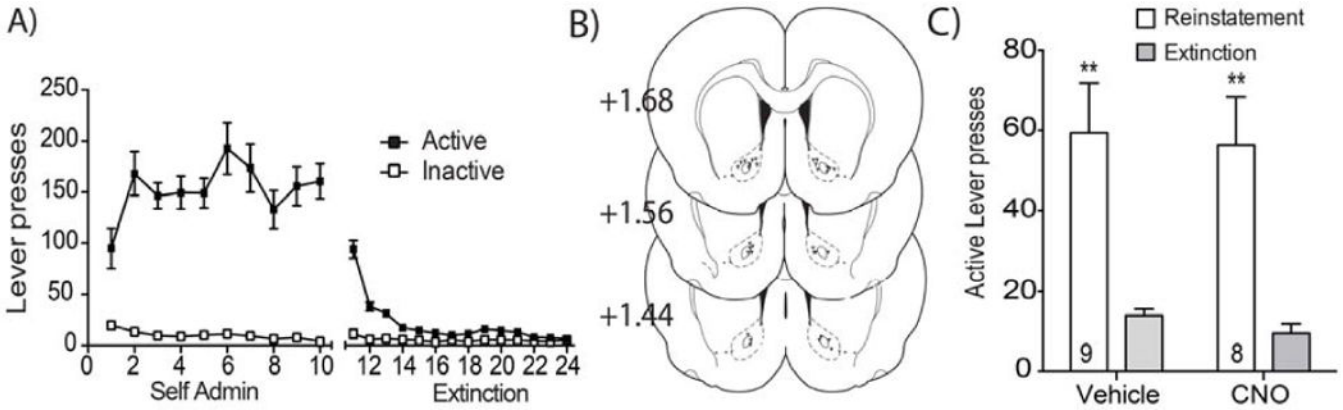

Figure 5. CNO activation of GFAP-Gq-DREADD in the NAcore had no effect on cue-induced reinstatement of sucrose seeking

A) Sucrose SA and extinction data (X-axis is days). **B)** Injection sites for rAAV5/GFAP-HA-hm3D-IRES-mCitrine viral infusion. The terminal points of virus injection sites are represented as small black triangles with the coordinates shown relative to bregma. **C)** Active lever presses for extinction and reinstatement for vehicle and CNO groups. Two-way repeated measures ANOVA revealed no significant effect of CNO treatment ($F_{(1, 15)}$=0.174; p=0.682), significant reinstatement ($F_{(1, 15)}$=28.31, p<0.0001) and no significant interaction ($F_{(1, 15)}$= 0.008, p=0.930). Bonferroni posttests revealed that cue-induced reinstatement increased active lever responding significantly (compared to extinction) in the vehicle group, as well as the CNO group, ** p<0.01.

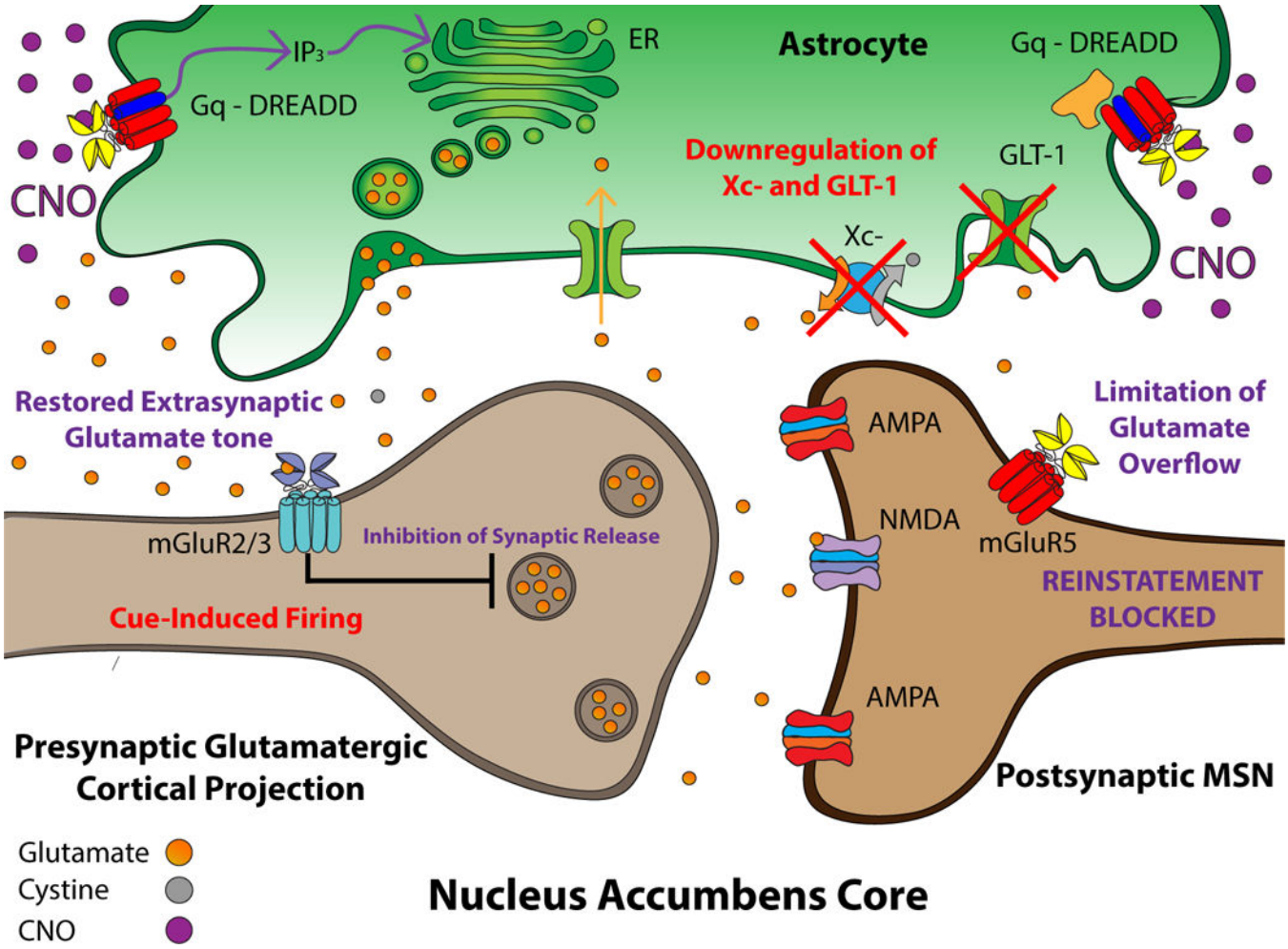

Figure 6. Summary of the mechanism of GFAP-Gq-DREADD-mediated reduction of cue-induced reinstatement

Following cocaine SA and extinction training, the cystine-glutamate exchanger (Xc-) is downregulated, contributing to reduced extracellular basal glutamate and decreased tone on presynaptic mGluR2/3 receptors (blue). Cocaine exposure also downregulates GLT-1 (green) which exacerbates glutamate overflow in response to cue exposure. Glutamate overflow normally activates postsynaptic glutamate receptors including mGluR5 (red), leading to the reinstatement of cocaine seeking. The activation of Gq-DREADD on astrocytes by CNO causes the production of IP_3, resulting in the release of Ca^{2+} from the endoplasmic reticulum (ER), leading to the vesicular release of glutamate. Glutamate release from astrocytes enhances extracellular glutamate concentration, restoring tone on presynaptic mGluR2/3 receptors which limits synaptic glutamate release, leading to lower levels of glutamate overflow and the inhibition of cue-induced cocaine seeking.